AIP | Review of Scientific Instruments

The response of CR-39 nuclear track detector to 1–9 MeV protons

N. Sinenian, M. J. Rosenberg, M. Manuel, S. C. McDuffee, D. T. Casey et al.

Citation: Rev. Sci. Instrum. **82**, 103303 (2011); doi: 10.1063/1.3653549
View online: http://dx.doi.org/10.1063/1.3653549
View Table of Contents: http://rsi.aip.org/resource/1/RSINAK/v82/i10
Published by the American Institute of Physics.

The response of CR-39 nuclear track detector to 1–9 MeV protons

N. Sinenian,[a] M. J. Rosenberg, M. Manuel, S. C. McDuffee,[b] D. T. Casey, A. B. Zylstra, H. G. Rinderknecht, M. Gatu Johnson, F. H. Séguin, J. A. Frenje, C. K. Li, and R. D. Petrasso[c]
Plasma Fusion Center, Massachusetts Institute of Technology, Cambridge, Massachusetts 02139-0001, USA

(Received 11 July 2011; accepted 6 September 2011; published online 28 October 2011)

The response of CR-39 nuclear track detector (TasTrak®) to protons in the energy range of 0.92–9.28 MeV has been studied. Previous studies of the CR-39 response to protons have been extended by examining the piece-to-piece variability in addition to the effects of etch time and etchant temperature; it is shown that the shape of the CR-39 response curve to protons can vary from piece-to-piece. Effects due to the age of CR-39 have also been studied using 5.5 MeV alpha particles over a 5-year period. Track diameters were found to degrade with the age of the CR-39 itself rather than the age of the tracks, consistent with previous studies utilizing different CR-39 over shorter time periods.
 [doi:10.1063/1.3653549]

I. INTRODUCTION

The detection of charged particles (and neutrons) using solid-state nuclear track detectors is of interest to many scientific disciplines, including the field of inertial confinement fusion (ICF) research; this includes both laser-plasma experiments[1–4] as well as Z-pinches.[5–10] In this context, CR-39 offers several advantages over alternative charged-particle detectors. As a passive, plastic detector, it is immune to electromagnetic pulse (EMP) and largely immune to x-rays which are commonly produced in such environments. For particles with normal incidence to the detector surface, the material has 100% detection efficiency for protons up to approximately 6–8 MeV. As will be described, this is accomplished using standard optical microscope techniques to image and analyze the detector.[11]

CR-39 has been used in wedge-range-filter and magnetic charged-particle spectrometers,[11] as well as neutron spectrometers using the recoil technique[12] at the OMEGA laser facility, and recently at the National Ignition Facility (NIF) for diagnosing neutrons and charged particles from ICF implosions.[13] CR-39 has also been fielded in a diagnostic for imaging ICF implosions,[14,15] which has allowed the detailed study of field structures in those experiments.[16,17] In these diagnostics, the track diameters are often used to discern different charged-particle species, and in several cases these are used to determine the energy of the incident particle. A thorough understanding of the response of CR-39 to charged particles is often important and sometimes essential for the success of such diagnostic instrumentation. Previous work, utilizing various types of CR-39, have studied the effectiveness of various track etchants,[18] and have looked at the CR-39 response to alpha particles,[19–21] electrons,[22] gammas,[23] fission fragments,[24] and neutrons.[25] Studies of the CR-39 efficiency for detecting protons as a function of incident angle in the energy range of 1–10 MeV have also been undertaken, as well as preliminary studies which characterized the track diameter as a function of incident mean proton energy.[24] In this work, we present the TasTrak®[26] CR-39 track diameter response curves to protons as a function of energy, including a study of piece-to-piece variability in addition to the effects of etch time and etchant temperature. We also present the results of a 5-year study of the effects of aging of CR-39 using 5.5 MeV alpha particles.

A charged particle leaves a track of broken molecular chains and free radicals along its trajectory as it passes through the plastic. Particle tracks are then made visible by chemical etching in hot, concentrated alkali solutions. The average diameter of the tracks left on the surface of the plastic will depend on the incident mean energy of the particles as well as how the CR-39 is processed. If the response of CR-39 to protons is understood for a range of etchant properties, we can obtain spectral information about the particles incident on the surface of the plastic.

This paper is structured as follows: Sec. II describes the principal experimental setup for this work; Sec. III presents the results of three different studies on CR-39's track diameter response, including piece-to-piece variability, effects of different etching conditions, and age of CR-39; Sec. IV describes the future direction of this work; Appendix illustrates how signal tracks are discerned from intrinsic noise for the different studies presented in this paper.

II. EXPERIMENTS

The studies presented in the following section involved exposing pieces of CR-39 to protons in the energy range of 0.92–9.28 MeV, which were produced using a linear accelerator-based fusion products generator.[27] A deuterium (D) ion beam was focused onto an erbium (Er) target embedded with either D or helium-3 (^{3}He) atoms to generate DD or D^{3}He fusion reactions. The 3 MeV DD-protons and 14.7-MeV D^{3}He-protons were used for the CR-39 exposure. Protons of the energy range indicated above were generated by overlaying the CR-39 with aluminum filters of various

[a]Electronic mail: nareg@psfc.mit.edu.
[b]Present address: Blue Sky Studios, Greenwich, Connecticut 06831, USA.
[c]Also a Visiting Senior Scientist at the Laboratory for Laser Energetics, University of Rochester, Rochester, NY, USA.

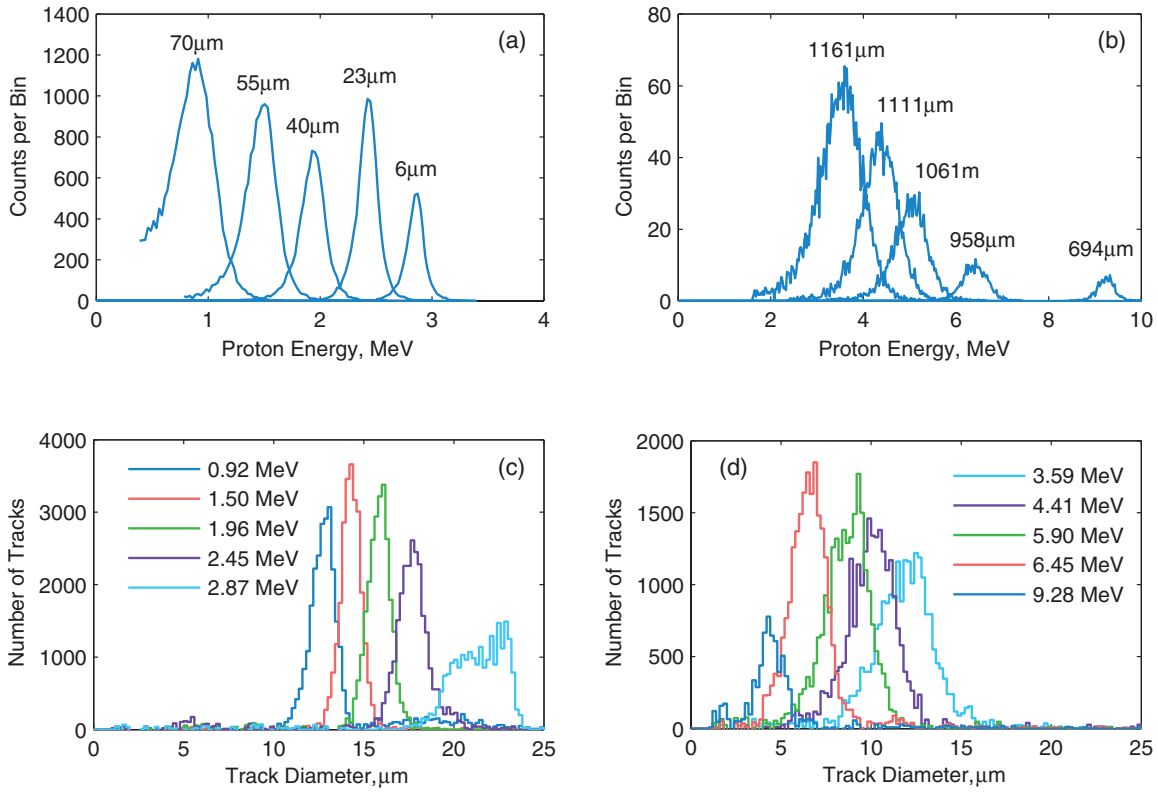

FIG. 1. (Color online) Energy distribution function of protons used in this study. Protons were generated from 3 MeV DD or 14.7 MeV D^3He fusion products with the use of stepped aluminum filters, which were overlaid on the CR-39 sample; filter thicknesses are indicated above respective peaks. Energy distributions were measured with a detector system utilizing a 2000 μm thick silicon surface barrier detector (SBD); the energy accuracy of the system was $\pm$75 keV.

thicknesses. The remaining charged fusion products (alphas and tritons) were readily ranged out with aluminum filters; the CR-39 response to the 2.45 MeV DD-neutron products is not of concern in this study since it has been demonstrated previously that the detection efficiency for these neutrons is approximately $(1.1 \pm 0.2) \times 10^{-4}$ on the front side of the CR-39 for a 6 h etch, and lower for shorter etch times.[25]

Measurements of the proton energy spectrum at birth as well as behind each individual aluminum filter were acquired using a silicon surface barrier detector (SBD) with a nominal depletion depth of 2000 μm, which is thick enough to completely stop 14.7-MeV protons. Two filter arrangements were constructed to range down the protons to the desired energies. The energy distribution of the protons leaving each of these filter packs was measured using an SBD (Fig. 1). Once the CR-39 was exposed to protons, it was etched using a heated solution of NaOH and then scanned with an automated optical microscope system, which recorded the location, diameter, eccentricity, and optical contrast of each track.[11] Following the scan, track attributes were analyzed using a custom software package developed at MIT.

III. RESULTS

A. Track diameter as a function of proton energy

The proton track diameter response of 1500-μm-thick CR-39 has been studied. Following exposure to protons, a 6*N* solution of NaOH at a temperature of 80 °C was used to etch the CR-39 for a duration of 6 h. A 6*N* solution of NaOH is typically used as it has been shown that the sensitivity of CR-39, defined here as the ratio between the etch rate of a track and that of the bulk (V_T/V_B), is maximized at this molarity;[28] higher sensitivity improves track contrast and the detection of charged particles with an optical microscope.

The diameter of proton tracks as a function of incident mean proton energy is shown in Fig. 2. The curves were acquired using two separate accelerator exposures, utilizing the two filter packs characterized in Figs. 1(a) and 1(b), on a single piece of CR-39, simply to avoid any piece-to-piece variation. The corresponding diameter distributions of protons behind each of the filters as recorded by the CR-39 are included for reference in Figs. 1(c) and 1(d). During exposure to 14.7 MeV protons, the upper portion of the CR-39, containing the thinner D-D aluminum filter pack, was blocked from the more energetic D-^{3}He protons using a vacuum shutter; this eliminated the need to vent the CR-39 to atmosphere and reconfigure filters, ensuring that the experiment was not perturbed between the two exposures. Eleven such exposures (Fig. 2(a)) were then made to characterize the piece-to-piece variability in the response. The average and standard deviation (dashed envelope) of these 11 exposures is shown in figure Fig. 2(b). It is important to note that the shape of each individual curve varies (see Fig. 2(a)); to use these curves quantitatively one must have knowledge of the shape of the curve for a given piece. It is thought that this piece-to-piece variation is a result of the variable oxygen profile of CR-39 upon irradiation.[29]

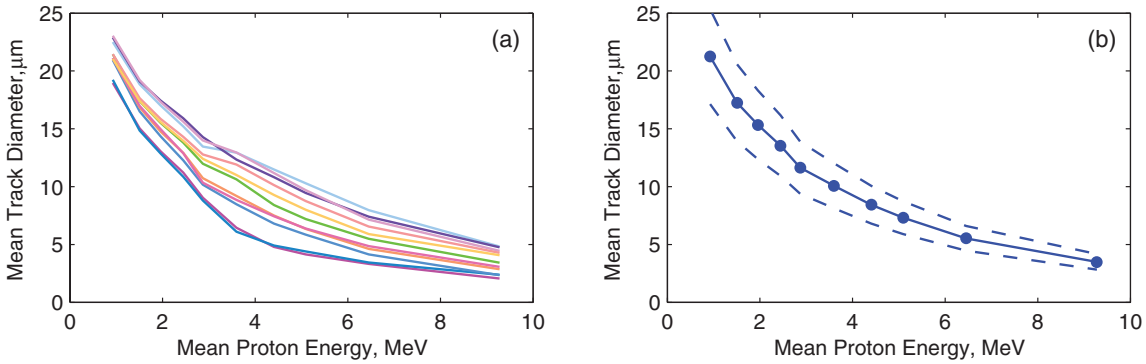

FIG. 2. (Color online) (a) Proton track diameter as a function of incident mean energy for TasTrak® CR-39 from 11 separate exposures; each piece was etched for 6 h in an 80 °C solution of 6 N NaOH. Variability in the shape of the curves from one piece to the next is observed. (b) Average (solid line) and standard deviation (dashed line) of proton track diameters as a function of incident mean energy computed using results from the 11 separate exposures of Fig. 2(a).

As illustrated in Fig. 2, the track diameters decrease with increasing incident mean proton energy, as expected from the stopping power scaling (dE/dx ∼ 1/E) of charged particles in cold matter. The features of these curves are in qualitative agreement with a previous study utilizing 1–10 MeV protons,[24] although that study used a different type of CR-39 (Homalite) as well as a different etchant (6 N at 70 °C).

In addition to these observed proton tracks, noise caused by defects and debris in the CR-39 are often observed. The diameters of these features, however, for the standard etch described above, are less than 2 μm and will not be counted as proton tracks for energies below 8 MeV.

B. Effects of etch time on track diameter

The effects of etch time were studied using four pieces of CR-39, which were exposed to protons of various energies using the aforementioned procedure. Each piece was then etched using a 6 N solution of NaOH at a temperature of 80 °C and scanned several times, starting with a 30 min etch and increasing in increments up to a total 6 h. This procedure was repeated for a total of four pieces and the results averaged to eliminate piece-to-piece variation; the resulting diameter response curves are shown in Fig. 3.

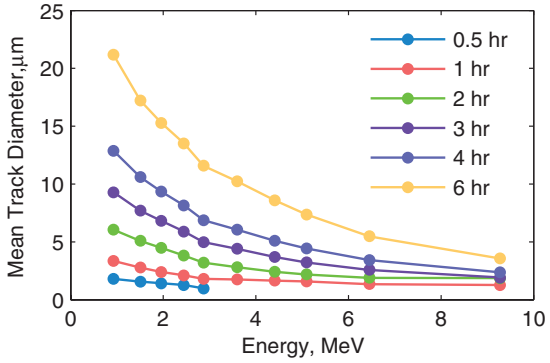

FIG. 3. (Color online) Proton track diameters as a function of incident mean energy for various etch times. Four samples of CR-39 were stage-etched in steps from 30 min up to 6 h in a 6 N NaOH solution at 80 °C; the results between the four pieces have been averaged to eliminate any piece-to-piece variation. A linear response between etch time and track diameter is demonstrated. Note that for a 30 min etch, protons with energies greater than 3 MeV are not detected, and hence, not shown.

In several charged-particle diagnostic "ICF" applications, the CR-39 in use often exhibits significant variations in the proton track density.[11,14] In such cases, it is desirable to apply a staged etch and scan process to the CR-39,[30] using scans from short and long etch times for regions of high and low fluence, respectively; for regions of high fluence this avoids track overlap and in severe cases complete saturation. It is important to etch regions of low fluence up to 6 h for these etch conditions so as to increase the contrast of proton tracks relative to the background intrinsic noise and improve counting statistics; for regions of higher fluence, statistics are not of concern and a shorter etch is tolerable. The fact that the 6-h etch in the staged etch of Fig. 3 is consistent with the single 6-h etch of Fig. 2 allows CR-39 processing in stages without affecting the response, thereby increasing the effective dynamic range in proton fluence.

C. Effects of etch temperature on track diameter

Previous work involved studies of the effects of etchant temperature variation on the CR-39 track diameter response to 1 MeV protons[31] as well as fission fragments and alpha particles.[18] These studies have been extended to include the track diameter response curves of protons in the energy range 1–9 MeV for various etchant temperatures (Fig. 4). The CR-

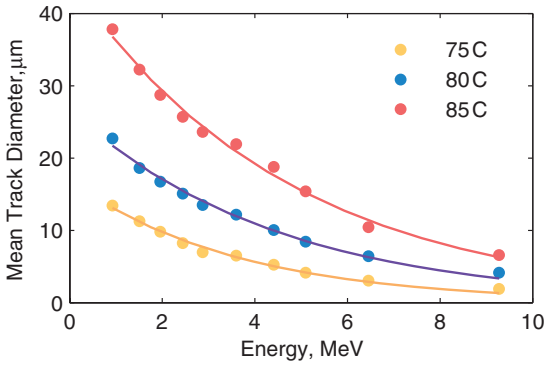

FIG. 4. (Color online) Proton track diameter as a function of incident mean energy for various etchant temperatures. Three separate pieces of CR-39 were exposed to protons and etched in a 6 N NaOH solution for 6 h at different etchant temperatures. Two exposures per piece were required to obtain each curve, as indicated by the accelerator shot numbers in the legend.

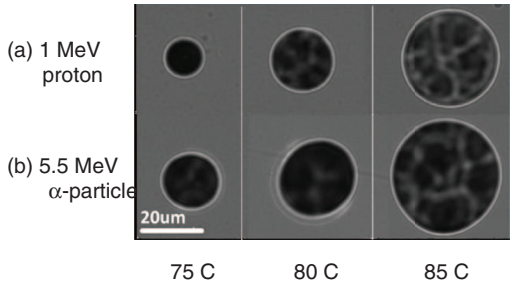

FIG. 5. Microscope images (at 40× magnification) of (a) 1 MeV proton and (b) 5.5 MeV alpha particle tracks on CR-39, illustrating the non-uniformity of track contrast with increasing etchant temperature. Images were taken from three samples, each containing protons and alphas.

39 for this study was etched for 6 h in a 6 N solution of NaOH at temperatures of 75, 80, and 85 °C.

Figure 4 shows that proton track diameters grow nearly linearly for these range of temperatures. Although higher etchant temperatures are clearly desirable from a processing standpoint (due to the reduced processing time) one must consider the integrity of the charged-particle tracks. Typical tracks of 1 MeV protons and 5.5 MeV alphas for these etchant temperatures, taken with an optical microscope (Fig. 5), show the loss of uniformity in track contrast over the surface of the track. It is unclear whether the loss of uniformity is due to temperature effects alone; this is also observed when etching CR-39 for longer times, due to etching beyond the end of the track.

D. Effects of aging and time of exposure

It has been shown previously that the CR-39 response to charged-particles drops sharply within the first 30 days of manufacture,[31] and that it is the age of the plastic itself, not of the tracks, which results in the degradation of sensitivity (lower V_T/V_B) with time.[32] The effects of prolonged aging on the CR-39 were studied using 5.5 MeV alpha particles from a ^{241}Am source and samples over a 5-year period. After exposure, samples were stored in a low-humidity, low-light environment at room temperature for a variable amount of time, after which they were etched using the standard 6 N solution of NaOH at 80 °C for 6 h. The diameters of the alpha tracks were found to decrease as a function of time between exposure and etch, as shown in Fig. 6(a). To determine whether it is the age of the plastic or the age of the track which causes a reduction in track diameter, another set of samples which were previously exposed to alpha particles were exposed again immediately before etch. The ratios of diameters of the "old" alpha tracks to the "new" alpha tracks is unity to within 5%, suggesting that it is the age of the CR-39, not the age of the track, which is responsible for the reduction in diameter, in agreement with previous claims utilizing different materials.[32] The cause for the observed change in response may be annealing[33] or oxidation.[32] Given the experimental setup, we rule out long-term exposure to UV and humidity. It has been shown that storing CR-39 at or below freezing temperatures will inhibit these aging effects.[32]

IV. SUMMARY AND FUTURE WORK

The response of TasTrak® CR-39 to 1–9 MeV protons has been studied, including the piece-to-piece variability of the response and the effects of different etch times and etchant temperatures. It has been shown that the shape of the proton track diameter vs. energy response curve varies from one piece to the next, and that quantitative use of these curves requires one to have knowledge of the shape of the curve for a given piece. Furthermore, a linear relationship between etch time and track diameter is observed, allowing for staged-etch processing of CR-39. Effects due to the age of CR-39 have also been studied over a 5-year period and from these experiments it was found that 5.5 MeV alpha particle track diameters decrease as a function of age of the plastic itself and not the age of the track. These characterizations of the response of CR-39 to protons are essential for the calibration of existing diagnostics and for the development of new diagnostic capabilities for the OMEGA and NIF laser facilities.

Future work will include the study of various environmental effects important to the ICF community. The effect on track diameters of prolonged exposure of CR-39 to vacuum both before and after exposure to protons has proven to be important at large facilities, such as the NIF where CR-39 may sit in vacuum for several hours, if not days, before

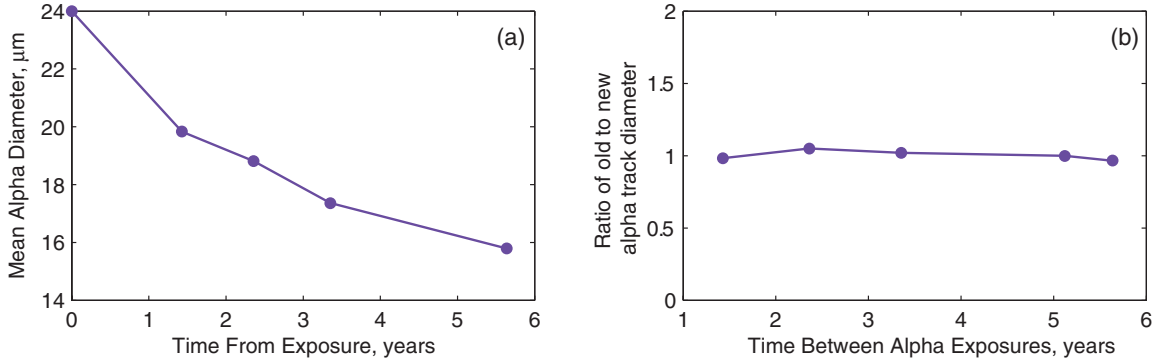

FIG. 6. (Color online) (a) Track diameter of alpha particles as a function of time between exposure of CR-39 pieces to 5.5 MeV alphas and etching. Each of these pieces was kept at room temperature with minimal exposure to light for the time periods shown. (b) The effects of aging on alpha-track diameter are independent on the time of exposure. CR-39, which had been previously exposed to alpha particles, was exposed again to alpha particles just prior to etching. The differences between new and old track diameters are ~5%.

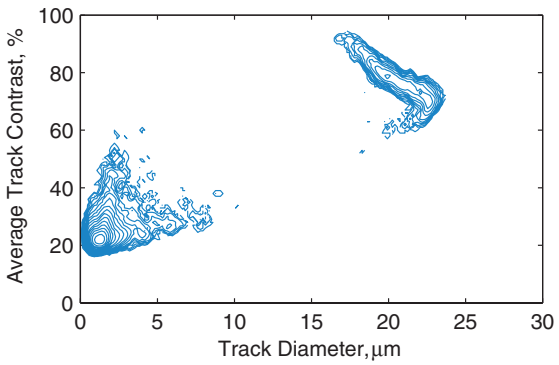

FIG. 7. (Color online) Contours of constant number of tracks as a function of track contrast and diameter for DD-p fusion products ranged down to 920 keV. The proton tracks are in the top right corner of the plot with intrinsic noise occupying regions of lower contrast and smaller diameter. Note how the diameter distribution turns around for these protons, resulting in the non-Gaussian diameter distribution of Fig. 1(c).

the experiment is begun.[29] The efficiency of track detection for shorter etch times and higher count rates (where track overlap becomes significant) is also of interest for improved processing turnaround time and increased flexibility in experiment designs, respectively. Finally, a detailed study of the x-ray response of CR-39 and in particular the effect of x-rays on charged-particle tracks will become important in the harsh x-ray environments of today's and tomorrow's increasingly more intense laser systems.

ACKNOWLEDGMENTS

The authors would like to thank Jocelyn Schaeffer, Robert Frankel, and Michelle Burke for etching and scanning the CR-39 used in this work. Also, we would like to thank Robert A. Childs and Sam Roberts for the many different ways they have contributed. The work described here was done in part for the author's PhD thesis, and was supported

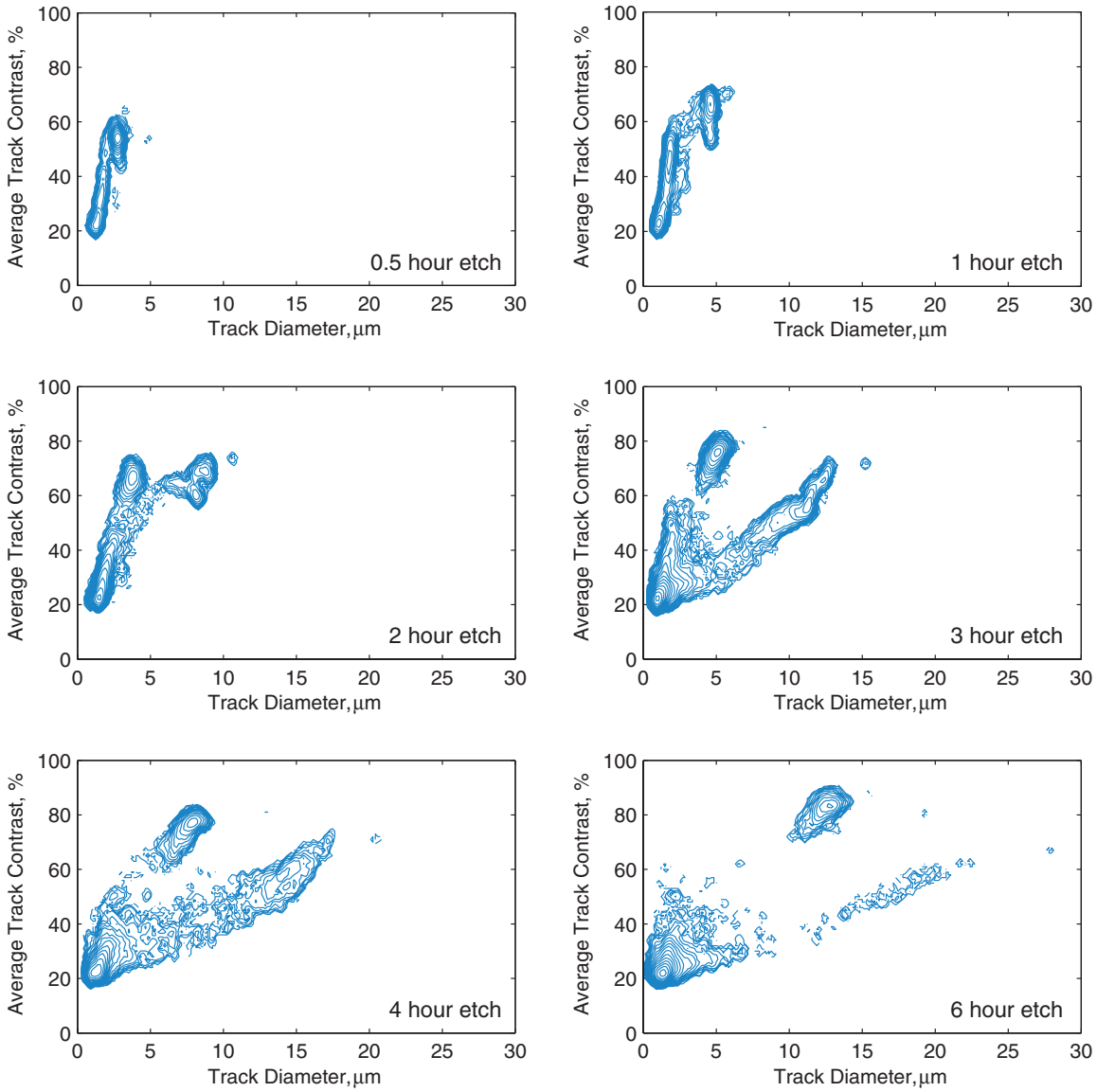

FIG. 8. (Color online) Contours of constant number of proton tracks as a function of track contrast and diameter for a single piece of CR-39 etched in stages. Shown are data for 2.9 MeV protons generated by ranging down D-^{3}He fusion protons with the use of aluminum filters. As the etch time is increased, the proton tracks shift towards higher contrast and larger diameters, making them more distinct from intrinsic noise.

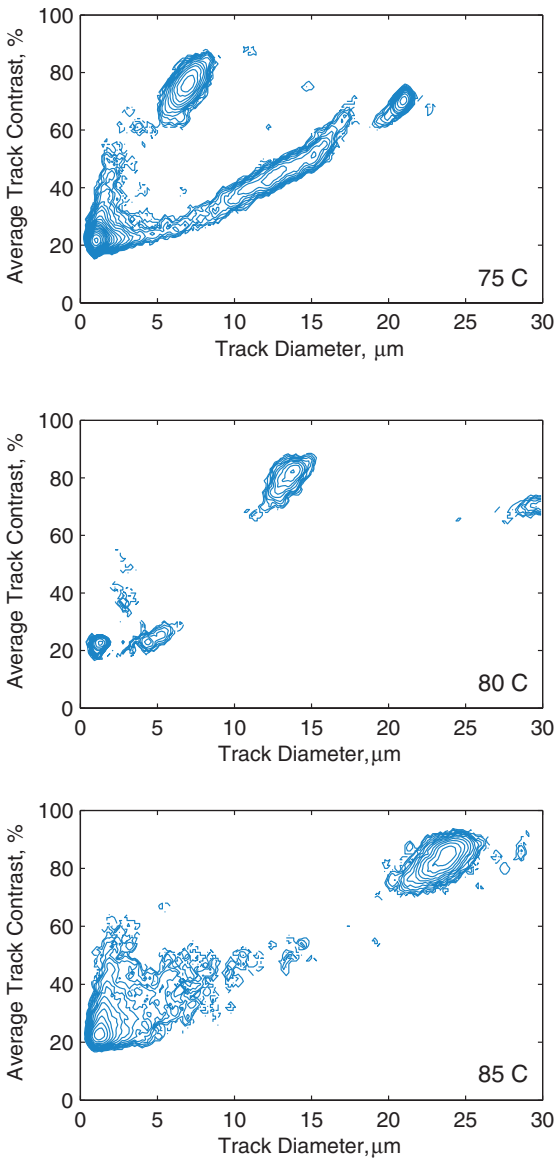

FIG. 9. (Color online) Contours of constant number of tracks as a function of track contrast and diameter for a 6 h etch at 75, 80, and 85 °C of 6 N NaOH. Two distinct islands of contours are visible in each plot: "noise" which occupies the bottom-left corner of contrast-diameter space and proton tracks which occupy the upper region and shift to the right for increasing etch temperatures.

in part by the National Laser Users' Facility (DOE Award No. DE-NA0000877), the Fusion Science Center (Rochester Sub-Award PO No. 415023-G), the U. S. Department of Energy (U.S. DOE) (Grant No. DE-FG03-03SF22691), the Laboratory for Laser Energetics (No. 412160-001G), Lawrence Livermore National Laboratory (No. B504974), and General Atomics under DOE (DE-AC52-06NA27279).

APPENDIX: VARIATION OF TRACK CONTRAST AND DIAMETER

The analysis of the CR-39 depends on careful discrimination of tracks based on a number of properties, including diameter, contrast, and eccentricity. The selection of signal tracks based on these properties is important in preferentially discriminating against noise. This appendix illustrates how the contours of constant numbers of signal tracks as a function of both diameter and contrast vary for the studies presented in this paper. Also included is a summary table of the accelerator shot numbers corresponding to the experiments in this study.

TABLE I. Accelerator shot numbers associated with the data shown in each of the figures.

Figure	MIT linear electrostatic accelerator (LEIA) reference shot number
Figure 1	A2010070801-A2010081005, A2010090801-A2010090804
Figure 2	A2010071201-A2010071202, A2010082003-A2010082004, A2010081903-A2010081904, A2010082007-A2010082008, A2010082704-A2010082705, A2010083001-A2010083002, A2010091001-A2010091002, A2010091003-A2010091004, A2010090801-A2010090802, A2010090803-A2010090804
Figures 3 and 8	A2010091001-A2010091004, A2010090801-A2010090804
Figures 4, 5, and 9 (75 °C)	A2011011401, A2011011402
Figures 4, 5, and 9 (80 °C)	A2011011403, A2011011404
Figures 4, 5, and 9 (85 °C)	A2011011405, A2011011406

1. Variation of contrast and diameter for low-energy protons

Figure 7 illustrates how track diameters of protons behave for proton energies near the Bragg peak of energy deposition in CR-39. The 920 keV protons in this case occupy the top-right corner of contrast vs. diameter space. Since protons with these energies are right near the Bragg peak for energy loss in CR-39, the diameters are no longer monotonic with energy, and hence, wrap around back to lower diameters. This results in the non-Gaussian diameter distribution shown in Fig. 1(c).

2. Variation of contrast and diameter with etch time

Figure 8 shows the variation of track contrast and diameter distributions with etch time for 2.9 MeV protons; these contrast and diameter distributions correspond to the data shown in Fig. 3. The low contrast, small diameter contours in the lower left of each plot show the intrinsic noise on the sample. As the etch time grows, the contours representing protons move towards larger diameters and higher contrast, making them easier to discern from the intrinsic background.

3. Variation of contrast and diameter with etch temperature

Shown in Fig. 9 are contours illustrating the diameter and contrast distributions for 2.9 MeV protons as a function

of etchant temperature. Increasing the etchant temperature shows effects similar to that of increasing etch time—proton tracks tend to become darker and larger since the etch rate is accelerated. Note the variation of the intrinsic noise between shown for the three etchant temperatures—this illustrates the variation of noise from piece-to-piece since three distinct samples were used to obtain the data.

4. Accelerator shot and CR-39 identification numbers

Table I shows the accelerator shot number reference and the CR-39 identification numbers associated with each of the data sets. The CR-39 used in this study was acquired in December 2009 and experiments were performed within a couple of months thereafter. The CR-39 was kept frozen and typically thawed for 24 h before it was used.

[1]R. L. McCrory, R. E. Bahr, R. Betti, T. R. Boehly, T. J. B. Collins, R. S. Craxton, J. A. Delettrez, W. R. Donaldson, R. Epstein, J. Fenje, V. Y. Glebov, V. N. Goncharov, O. V. Gotchev, R. Q. Gram, D. R. Harding, D. G. Hicks, P. A. Jaanimagi, R. L. Keck, J. H. Kelly, J. P. Knauer, C. K. Li, S. J. Loucks, L. D. Lund, F. J. Marshall, P. W. McKenty, D. D. Meyerhofer, S. F. B. Morse, R. D. Petrasso, P. B. Radha, S. P. Regan, S. Roberts, F. Séguin, W. Seka, S. Skupsky, V. A. Smalyuk, C. Sorce, J. M. Soures, C. Stoeckl, R. P. J. Town, M. D. Wittman, B. Yaakobi, and J. D. Zuegel, Nucl. Fusion **41**(10), 1413 (2001).

[2]G. H. Miller, E. I. Moses, and C. R. Wuest, Nucl. Fusion **44**(12) (2004).

[3]T. C. Sangster, R. L. McCrory, V. N. Goncharov, D. R. Harding, S. J. Loucks, P. W. McKenty, D. D. Meyerhofer, S. Skupsky, B. Yaakobi, B. J. MacGowan, L. J. Atherton, B. A. Hammel, J. D. Lindl, E. I. Moses, J. L. Porter, M. E. Cuneo, M. K. Matzen, C. W. Barnes, J. C. Fernandez, D. C. Wilson, J. D. Kilkenny, T. P. Bernat, A. Nikroo, B. G. Logan, S. Yu, R. D. Petrasso, J. D. Sethian, and S. Obenschain, Nucl. Fusion **47**, S686 (2007).

[4]M. Tabak, J. Hammer, M. E. Glinsky, W. L. Kruer, S. C. Wilks, J. Woodworth, E. M. Campbell, M. D. Perry, and R. J. Mason, Phys. Plasmas **1**(5), 1626 (1994).

[5]X. M. Guo and C. M. Luo, J. Phys. D **29**(2), 388 (1996).

[6]F. Castillo Mejía, M. Milanese, R. Moroso, and J. Pouzo, J. Phys. D **30**(10), 1499 (1997).

[7]E. Skladnik-Sadowska, J. Baranowski, K. Kolacek, A. Kishinets, A. A. Rupasov, M. Ripa, P. Ctibor, M. J. Sadowski, B. Sartowska, and A. Szydlowski, Radiat. Meas. **36**(1), 321 (2003).

[8]S. V. Springham, T. H. Sim, P. Lee, A. Patran, R. S. Rawat, P. M. E. Shutler, T. L. Tan, and S. Lee, Phys. Scr. **2006**(T123), 124 (2006).

[9]R. Verma, M. V. Roshan, F. Malik, P. Lee, S. Lee, S. V. Springham, T. L. Tan, M. Krishnan, and R. S. Rawat, Plasma Sources Sci. Technol. **17**(4), 045020 (2008).

[10]M. Zakaullah, I. Akhtar, A. Waheed, K. Alamgir, A. Z. Shah, and G. Murtaza, Plasma Sources Sci. Technol. **7**(2), 206 (1998).

[11]F. H. Séguin, J. A. Frenje, C. K. Li, D. G. Hicks, S. Kurebayashi, J. R. Rygg, B. E. Schwartz, R. D. Petrasso, S. Roberts, J. M. Soures, D. D. Meyerhofer, T. C. Sangster, J. P. Knauer, C. Sorce, V. Y. Glebov, C. Stoeckl, T. W. Phillips, R. J. Leeper, K. Fletcher, and S. Padalino, Rev. Sci. Instrum. **74**(2), 975 (2003).

[12]J. A. Frenje, D. T. Casey, C. K. Li, F. H. Seguin, R. D. Petrasso, V. Y. Glebov, P. B. Radha, T. C. Sangster, D. D. Meyerhofer, S. P. Hatchett, S. W. Haan, C. J. Cerjan, O. L. Landen, K. A. Fletcher, and R. J. Leeper, Phys. Plasmas **17**(5), 056311 (2010).

[13]J. A. Frenje, D. T. Casey, C. K. Li, F. H. Seguin, R. D. Petrasso, V. Y. Glebov, P. B. Radha, T. C. Sangster, D. D. Meyerhofer, S. P. Hatchett, S. W. Haan, C. J. Cerjan, O. L. Landen, K. A. Fletcher, and R. J. Leeper, Phys. Plasmas **17**, 056311 (2010).

[14]J. R. Rygg, F. H. Séguin, C. K. Li, J. A. Frenje, M. J. -E. Manuel, R. D. Petrasso, R. Betti, J. A. Delettrez, O. V. Gotchev, J. P. Knauer, D. D. Meyerhofer, F. J. Marshall, C. Stoeckl, and W. Theobald, Science **319**(5867), 1223 (2008).

[15]F. H. Séguin, J. L. DeCiantis, J. A. Frenje, S. Kurebayashi, C. K. Li, J. R. Rygg, C. Chen, V. Berube, B. E. Schwartz, R. D. Petrasso, V. A. Smalyuk, F. J. Marshall, J. P. Knauer, J. A. Delettrez, P. W. McKenty, D. D. Meyerhofer, S. Roberts, T. C. Sangster, K. Mikaelian, and H. S. Park, Rev. Sci. Instrum. **75**(10), 3520 (2004).

[16]C. K. Li, F. H. Seguin, J. A. Frenje, M. Rosenberg, R. D. Petrasso, P. A. Amendt, J. A. Koch, O. L. Landen, H. S. Park, H. F. Robey, R. P. J. Town, A. Casner, F. Philippe, R. Betti, J. P. Knauer, D. D. Meyerhofer, C. A. Back, J. D. Kilkenny, and A. Nikroo, Science **327**(5970), 1231 (2010).

[17]C. K. Li, F. H. SÈguin, J. A. Frenje, J. R. Rygg, R. D. Petrasso, R. P. J. Town, P. A. Amendt, S. P. Hatchett, O. L. Landen, A. J. Mackinnon, P. K. Patel, V. A. Smalyuk, T. C. Sangster, and J. P. Knauer, Phys. Rev. Lett. **97**(13), 135003 (2006).

[18]Matiullah, S. Rehman, S. Rehman, and W. Zaman, Radiat. Meas. **39**, 7 (2005).

[19]K. F. Chan, B. M. F. Lau, D. Nikezic, A. K. W. Tse, W. F. Fong, and K. N. Yu, Nucl. Instrum. Methods Phys. Res. B **263**(1), 290 (2007).

[20]A. P. Fews and D. L. Henshaw, Nucl. Instrum. Methods Phys. Res. **197**(2–3), 517 (1982).

[21]A. P. Fews and D. L. Henshaw, Nucl. Instrum. Methods Phys. Res. **223**(2–3), 609 (1984).

[22]J. Charvát and F. Spurný, Int. J. Radiat. Appl. Instrum. D. **14**(4), 451 (1988).

[23]N. E. Ipe and P. L. Ziemer, Radiat. Prot. Dosimetry **14**(3), 237 (1986).

[24]H. A. Khan, R. Brandt, N. A. Khan, and K. Jamil, Nucl. Tracks Radiat. Meas. **7**(3), 129 (1983).

[25]J. A. Frenje, C. K. Li, F. H. Seguin, D. G. Hicks, S. Kurebayashi, R. D. Petrasso, S. Roberts, V. Y. Glebov, D. D. Meyerhofer, T. C. Sangster, J. M. Soures, C. Stoeckl, C. Chiritescu, G. J. Schmid, and R. A. Lerche, Rev. Sci. Instrum. **73**(7), 2597 (2002).

[26]T. A. S. L., See http://www.tasl.co.uk/ for more information on TasTrak® CR-39.

[27]S. C. McDuffee, J. A. Frenje, F. H. Seguin, R. Leiter, M. J. Canavan, D. T. Casey, J. R. Rygg, C. K. Li, and R. D. Petrasso, Rev. Sci. Instrum. **79**(4), 043302 (2008).

[28]S. A. Durrani and R. K. Bull, *Solid State Nuclear Track Detections, Principles, Methods and Applications* (Pergamon, New York, 1987).

[29]M. J.-E. Manuel, M. J. Rosenberg, N. Sinenian, H. Rinderknecht, A. B. Zylstra, F. H. Séguin, J. Frenje, C. K. Li, and R. D. Petrasso, Rev. Sci. Instrum. **82**, 095110 (2011).

[30]D. T. Casey, J. A. Frenje, F. H. Séguin, C. K. Li, and M. J. Rosenberg, Rev. Sci. Instrum. **82**, 073502 (2011).

[31]B. G. Cartwright, E. K. Shirk, and P. B. Price, Nucl. Instrum. Methods **153** (2–3), 457 (1978).

[32]T. Portwood, D. L. Henshaw, and J. Stejny, Int. J. Radiat. Appl. Instrum. D **12**(1–6), 109 (1986).

[33]R. K. Bhatia, R. C. Singh, and H. S. Virk, Nucl. Instrum. Methods Phys. Res. B **46** (1–4), 358 (1990).